DOI: 10.1002/ejic.201000483

Classes of Nanomagnets Created from Alkanethiol-Coated Pt or Pd Nanoparticles and Their Alloys with Co

Akira Miyazaki,*[a,b] Yoshikazu Ito,[b] and Toshiaki Enoki*[b]

Keywords: Metal nanoparticles / Quantum-size effect / Metal-organic interface / Exchange enhancement / Single particle magnet

Alkanethiol-coated metal nanoparticles are fascinating materials for designing unconventional electronic and magnetic functions. Novel classes of magnetic nanosystems can be created using Pd and Pt nanoparticles and their alloys with a 3d transition metal using quantum size, interface and exchange enhancement effects. The charge transfer at the metal–organic interface and the quantum size effect render Pt and Pd nanoparticles magnetic with localised moments. The substitution of capping molecules with a TTF derivative having a long alkanethiol substituent decreases the totalspin concentration due to partial oxidation of the TTF units. Pd nanoparticles containing Co atoms as magnetic centres have significantly enhanced magnetic moments because of the exchange enhancement. Interestingly, in Pd nanoparticles of 2 nm in diameter containing only one Co atom per particle, the Co atom magnetises all of the Pd atoms in the particle. Therefore, the nanoparticles behave as a single nanoparticle magnet that shows blocking behaviour.

Introduction

Metal nanoparticles have attracted much attention in physics and chemistry, and are considered to be essential building blocks for the construction of nanosized devices of the next generation.[1] Various unconventional properties and functionalities of nanoparticles come primarily from their nanometre order particle size. In this sense, the peculiarities of nanoparticles should be discussed in terms of size effects. In addition, when the surface of a nanoparticle is covered with other chemical species, the interface created between the metal core and the covering shell can play a role in giving various functionalities depending on how the shell interacts with the metal core. For example, chemical

[a] Department of Environmental Applied Chemistry, University of Toyama,
3190 Gofuku, Toyama-shi 930-8555, Japan
Fax: +81-76-445-6824
E-mail: miyazaki@eng.u-toyama.ac.jp
[b] Department of Chemistry, Tokyo Institute of Technology,
2-12-1-W4-1 O-okayama, Meguro-ku 152-8551, Japan
Fax: +81-3-5734-2242
E-mail: enoki.t.aa@m.titech.ac.jp

Akira Miyazaki was born in Niigata, Japan, and received his Ph. D degree in multi-disciplinary sciences from the University of Tokyo under the direction of Tadashi Sugawara. In 1993, he joined Prof. Enoki's research group as an Assistant Professor, and in 2008, he was appointed to the position of Associate Professor in the Department of Environmental Applied Chemistry at University of Toyama. His research field is the development and characterization of inorganic–organic composite materials such as molecular materials and metal nanoparticles showing electrical conductivity and magnetism.

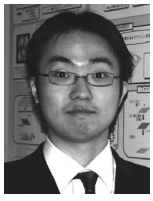

Yoshikazu Ito received his MS degree in Department of Chemistry from Tokyo Institute of Technology (2009) and is now a PhD student there under the supervision of Prof. Toshiaki Enoki. His main research topic is the synthesis and characterization of size- and composition-controlled Pd-based alloy magnetic nanoparticles and their functionalization from the perspectives of magnetism and magnetic catalysis. He obtained a JPSP fellowship in 2009.

Toshiaki Enoki was born in 1946, and received his Ph.D. in 1974 from Kyoto University, Japan, under the supervision of Prof. Ikuji Tsujikawa. In 1987, he was appointed to the position of Associate Professor in the Department of Chemistry at Tokyo Institute of Technology, and is now a full Professor. His research interests include the physical chemistry of molecular magnetism. He has been investigating molecular magnets based on organic charge transfer complexes and carbon nanomaterials. He has also been leading studies on magnetism in nanographenes, which have recently been recognised as important spintronics materials.

modifications of the nanoparticle surfaces can furnish functionalised supramolecular systems that are utilised in microchemical analysis.[2]

The effects of particle size on the electronic structure of metal nanoparticles can be classified into those of Coulomb blockade island and quantum size. The Coulomb blockade island effect is understood with classical electrodynamics. The Coulomb repulsion or charging energy caused by addition of an electron to a particle is expressed as $U = e^2/4\pi\varepsilon_0\varepsilon_r d$, where ε_r and d are the dielectric constant and particle diameter, respectively. For a particle with a diameter of 1 nm, this Coulomb repulsion energy (0.2 eV, 2300 K) greatly exceeds the thermal energy at room temperature (27 meV, 300 K). Therefore, nanoparticles can work as Coulomb blockade islands exhibiting the single-electron tunnelling effect even at room temperature. This has been demonstrated in the staircase-like current–voltage characteristics using scanning tunnelling spectroscopy,[3] and in the non-linear current–voltage characteristics of nanoparticles connected with molecular wires.[4]

The quantum size effect, on the other hand, is a quantum mechanical effect. The energy discreteness δ of molecular orbitals is on the order of electron volts and greatly exceeds the thermal energy k_BT, whereas bulk metals have a continuous density of states and δ is orders of magnitude smaller than k_BT. As the dimensions of metal nanoparticles lie between these two extremes, the energy discreteness δ can be of the same order as the thermal energy k_BT as illustrated in Figure 1. In fact, δ is theoretically approximated as E_F/N where E_F is the Fermi energy of the metal and N is the number of atoms per particle.[5] Thus, δ often becomes comparable to the thermal energy in metal nanoparticles. Therefore, the conduction electrons of metal nanoparticles, which are delocalised at high temperatures and show weak Pauli paramagnetism similar to bulk metals, can possess localised natures at low temperatures. As a result, an individual metal nanoparticle becomes paramagnetic with localised magnetic moments when it contains an odd number of electrons.[5a]

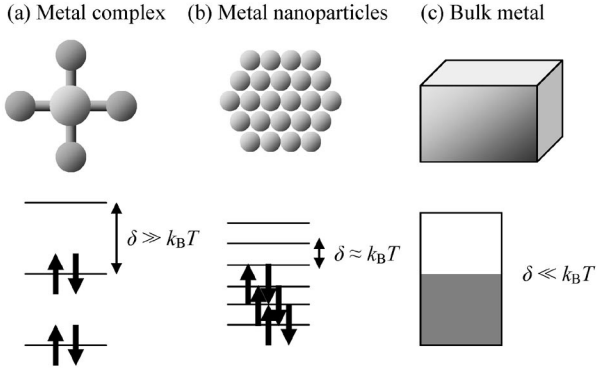

Figure 1. Illustrations of the energy discreteness in (a) a metal complex, (b) a metal nanoparticle and (c) bulk metal.

The behaviours of magnetic nanoparticles such as Co or Fe are also different from those of their bulk forms and strongly affected by their particle size.[6] There are two important size effects to be considered; the single-domain limit and superparamagnetic behaviour. The single-domain limit is observed in ferromagnetic (or ferrimagnetic) nanoparticles. In bulk ferromagnetic materials the magnetic domain structure is thermodynamically preferable, as a consequence of the balance between the magnetostatic energy proportional to the domain size and the domain-wall energy proportional to the domain boundary area. If the particle size is reduced below the single-domain limit (on the order of 10 nm depending on the material),[6b] the domain-wall energy exceeds the magnetostatic energy and the multi-domain structure becomes thermodynamically unfavourable. The resulting single-domain nanoparticles are uniformly magnetised with all magnetic moments aligned in the same direction. Therefore, very high coercive force is observed in an array of single domain ferromagnetic nanoparticles.

Superparamagnetic behaviour is observed when ferromagnetic nanoparticles are sufficiently isolated from each other by a non-magnetic medium. The energy required to reverse the magnetization (magnetic moment) of a single-domain particle is proportional to KV/k_BT, where K is the magnetic anisotropy constant and V is the particle volume. If the thermal energy k_BT is larger than this barrier energy, the magnetization is easily reversed by an external magnetic field. More precisely, if the temperature is high enough the relaxation time τ of the magnetic moment of a particle given by $\tau = \tau_0 \exp(KV/k_BT)$ is sufficiently small. As a result, the magnetic moment of this particle behaves like that of a conventional paramagnetic species as shown in Figure 2, except that the spin multiplicity per particle is enor-

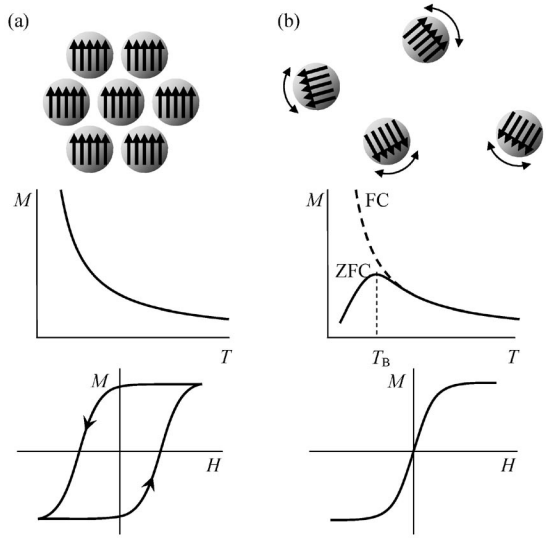

Figure 2. An illustration of the temperature dependence of magnetic moments (middle) and magnetization curves (lower) in (a) an array of ferromagnetic nanoparticles and (b) isolated superparamagnetic nanoparticles. FC and ZFC denote field-cooling and zero-field cooling, respectively.

mously large. Therefore, this high-temperature state is called a superparamagnetic state. In the low-temperature region the reversal magnetic moment becomes slower than the time scale of measurement, and the magnetic susceptibility depends on whether the system is cooled in the presence (field cooling) or absence (zero-field cooling) of the magnetic field. This low-temperature state, which shows a dependence on the cooling condition (Figure 2), is referred as a blocked state. The temperature that separates the superparamagnetic state and the blocked state is defined as blocking temperature (T_B).

The typical and most intensively investigated metal nanoparticles are gold nanoparticles.[7] Although colloidal gold was already known and used in the Roman Empire for making ruby glass, the scientific history of Au nanoparticles only began in the latter half of the 20th century, especially after the pioneering works of Schmid's Au_{55} clusters.[8] The most remarkable breakthrough has been the report of the Brust–Schiffrin method, which uses alkanethiols as capping molecules[9] and easily yields stable Au nanoparticles with narrow particle size distributions. Due to the high affinity between Au (a soft Lewis acid) and S (a soft Lewis base), gold nanoparticles covered with alkanethiols are the most stable metal nanoparticles, and their electronic, magnetic and optical properties have been investigated in detail.[7] Nowadays, Au nanoparticles are widely used in various biochemical and medical applications including protein immobilization[10] and drug delivery.[11]

We consider, however, platinum (Pt) and especially palladium (Pd) nanoparticles as more fascinating targets in light of their electronic and magnetic structures. Like Au, Pt and Pd also have high affinity to sulfur, which promises the formation of stable nanoparticles coated with alkanethiols. Pt and especially Pd have narrow bandwidths and hence a high density of states at their Fermi energies due to the contributions of *d* orbitals.[12] This indicates that the electronic state is sensitive to changes in the Fermi level. As a result, the electronic state of nanoparticles can be easily modified with small perturbations from the external environment. It has also been pointed out that Pd alloys containing magnetic transition metal atoms such as Co have giant magnetic moments,[13] as a consequence of the exchange interaction between the conduction electrons of Pd and the localised moments on the magnetic transition-metal atoms.

In this microreview, we deal with platinum and palladium nanoparticles investigated by our group focusing on their electronic and magnetic properties. First we discuss the interface effect on the electronic structure of alkanethiol-coated Pt and Pd nanoparticles, where the organic layers play also an important role in the electronic structure of the metal core-organic shell systems. We then discuss the magnetic properties of Pd nanoparticles containing Co atoms as paramagnetic centres. Here we observe their large magnetic moments caused by the exchange enhancement mechanism,[14] and their magnetic behaviours which characterise them as single-particle magnets.

Interface Effects on the Electronic Structure of Metal Nanoparticles Covered with Alkanethiol Layers

Alkanethiol-Coated Platinum Nanoparticles

As discussed in the introduction, the electronic properties of metal nanoparticles are an important target of condensed matter physics in light of the quantum size and Coulomb blockade island effects. The surface of such nanoparticles is often covered with a chemically inert organic layer working as a stabiliser. Without this organic layer, the metal particles easily aggregate and grow into particles with larger dimensions. Many small molecular ligands,[8,15] surfactants[16] and polymers[17] have been used to protect particles from aggregation by coating their surface. If the chemical interaction between the core nanoparticles and the surrounding organic layer is sufficiently strong, not only can the coating layer control the size of the nanoparticles, but it can also affect their physical properties. However, the effects of these coating layers on the electronic structure of the nanoparticles have not been well recognised.

Here we focus on the electronic structure of alkanethiol-coated Pt nanoparticles [18] for the following reasons. Alkanethiol is known to be a good stabiliser for metal nanoparticles such as Au, Pd and Pt, and there are several convenient one-pot synthetic methods to obtain alkanethiol-stabilised metal nanoparticles.[9,19] In such systems the terminal –SH group of the alkanethiol molecule is replaced by a sulfur–metal atom bond. It is therefore expected that this covalent character between the core metal particle and the organic shell will give rise to unconventional electronic features, especially at the core-shell interface.

Octadecanethiol-coated Pt nanoparticles were prepared by chemical reduction of $H_2PtCl_6{\cdot}6H_2O$ using a strong reducing agent, lithium triethylborohydride (superhydride), in the presence of octadecanethiol as a capping molecule. The more abundant the octadecanethiol molecule, the smaller were the obtained particles. The structure inside the nanoparticles was elucidated with high-resolution TEM photographs and electron diffraction patterns. The TEM image of a nanoparticle clearly shows the interior lattice pattern (Figure 3), indicating a regular atomic alignment inside the particle. The electron diffraction pattern shows the face-centred cubic (fcc) lattice with a lattice constant similar to

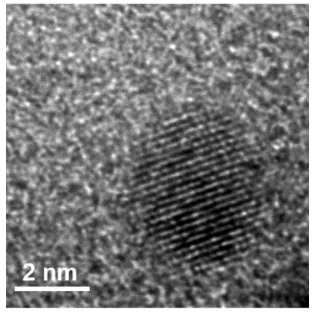

Figure 3. High-resolution TEM photograph for Pt nanoparticles having an average diameter of 1.15 nm.

that of bulk Pt metal. Assuming a spherical shape for the particles, the average number of atoms per particle N is estimated to be between 30 and 200 for an average particle size between 0.93 and 1.78 nm.

The magnetic susceptibility χ of the Pt nanoparticles is expressed as the sum of a Curie term and a temperature-independent term. By subtracting the core diamagnetic contribution of the organic layer from the temperature-independent term, the Pauli paramagnetic susceptibility χ_0 of the Pt core is obtained, which is about one fifth of that of bulk Pt (0.98×10^{-6} emu g^{-1}) and decreases as the particle size is reduced (Figure 4, a). From the Curie term the spin concentration N_s is estimated to be about 0.5 spins per particle and nearly independent of particle size (Figure 4, b), indicating that about half of the nanoparticles contain an unpaired electron.

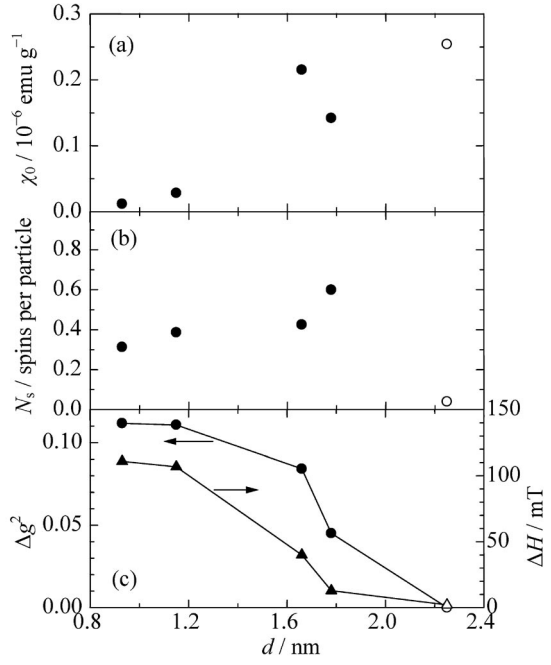

Figure 4. The particle diameter (d) dependence of (a) the Pauli paramagnetic susceptibility χ_0, (b) the spin concentration N_s and (c) the g-value [Δg^2 (circles)] and line width ΔH (triangles) in ESR spectra. The open symbols denote data for Pt nanoparticles without capping molecules.[21]

The reduction in Pauli paramagnetism and the emergence of the Curie term can be attributed to the quantum size effect. When the size of the system reaches the nanometre range, the energy discreteness δ becomes comparable to the thermal energy. In the present nanoparticle systems, the energy discreteness is estimated to increase from 0.025 to 0.35 eV as the particle size is lowered from 2.2 to 0.9 nm, thereby exceeding the thermal energy k_BT at room temperature (27 meV, 300 K) in smaller particles. The Pauli susceptibility is then given by $\chi_0 = 2\ \mu_B{}^2/\delta$ in the high temperature limit, whereas in the low temperature limit it either converges to zero or displays Curie-type divergence, respectively, for systems having an even or odd number of electrons.[5a] The observed Pauli paramagnetic susceptibility χ_0 is well reproduced by the quantum size effect with the estimated energy discreteness, suggesting the importance of this effect in the magnetic properties of Pt nanoparticles.

However, the nature of the Curie-type localised spin apparently disagrees with the electronic state of the Pt nanoparticles, which have an even number of electrons in their neutral state. Experimental findings ($N_s \approx 0.5$ spins per particle) show that about half of the nanoparticles should be in an odd electron system. Consistency can be achieved if the electronic deficiency or excess resulting from a charge transfer between the Pt core and organic shell is taken into account. In order to detect the interlayer charge transfer we measured the XPS spectra of Pt nanoparticles having an average diameter of 1.15 nm. The binding energies of Pt 4*f* electrons of the nanoparticles are found to be higher than those of bulk Pt, whereas the binding energy of S 2*p* is lower than that of pure octadecanethiol molecules. The origin of these peak shifts can be explained in terms of charge transfer from the Pt particle to the organic layer, consistent with the order of the electronegativity of these elements (Pt: 2.28, S: 2.58).[20] The charge transfer causes electron-deficient features in the electronic structure of the interior Pt nanoparticle, which in turn raises the binding energy of Pt 4*f* electrons. On the other hand, the sulfur atoms have electron-rich features and the binding energy of S 2*s* electrons becomes lower as a result of this core-to-shell partial charge transfer. The electron deficiency of the Pt core changes the electronic system from an even electron state to an odd electron state, resulting in the creation of localised magnetic moments as observed.

ESR measurements also give detailed insight into the location of the unpaired electrons. The squared g-value deviation Δg^2 [$= (g - g_0)^2$, $g_0 = 2.0023$ is the g-value of free electron spin] and the line width ΔH of the ESR absorption at room temperature are significantly larger than those in naked Pt nanoparticles.[21] These values are nearly independent of temperature and significantly rise as the mean particle diameter decreases (Figure 4, c). The large values for Δg^2 and ΔH and their similar trends as a function of particle size suggest a large enhancement of spin-orbit interaction. This ultimately tells us that spin-lattice relaxation in the electron spins occurs at the interface between the octadecanethiol-monolayer and the Pt core. In other words, the spin-lattice relaxation is accelerated by the enhancement of the spin-orbit interaction owing to the modification in the electronic structure at the interface. Indeed, the magnitude of the spin-orbit interaction ζ is expressed as $\zeta \propto \langle \nabla V(r)/r \rangle\ \rho(r, E_F)$, where $\nabla V(r)$ is the gradient of the electrostatic potential and $\rho(r, E_F) = |\psi(r, E_F)|^2$ is the local electron density at the Fermi level.[22] At the core-shell interface, the local electron density takes on a significant value due to bond formation at the metal–thiol interface where V varies abruptly, the spin-orbit interaction being remarkably enhanced. Theoretical estimation of the spin–lattice relaxation time from the ESR line width[23] also suggests that the quantum size effect for the core Pt particles plays an important role in this fast relaxation at the interface.

Pd Nanoparticles Coated with a TTF Derivative

In the previous section we have shown that the surface-covering organic layers act not only to protect the metal particles from aggregating but also to modify the electronic state of the metal nanoparticles themselves through partial charge transfer between the core and shell layer. It is therefore expected that by introducing electrochemically active molecules such as electron-donors or acceptor molecules in the covering layer, the electronic state of the metal core can be modified to tune the electronic and magnetic properties of the metal core-organic shell system.

Based on this view, we have introduced a TTF derivative having a long alkylthio substituent (Scheme 1) in the alkanethiol layer.[24] Indeed, TTF and its derivatives have been extensively used to create molecular conductors including superconductors.[25] Therefore, they can also participate in the electron-transferring process at the interface of self-assembled monolayer (SAM) films.[26] In this section we adopt Pd as a metal nanoparticle core. Since bulk Pd has a sharp density-of-states peak around the Fermi level due to the contribution of the d-electron levels,[12] it is expected that the interface effect associated with the charge transfer between the metal core and organic layer will emerge more sensitively in Pd nanoparticles than their Pt counterparts.

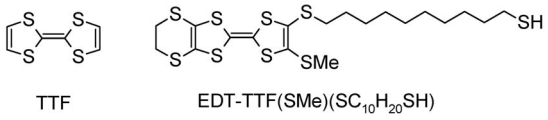

Scheme 1. Molecular structures of TTF and EDT-TTF(SCH_3)-($SC_{10}H_{20}SH$).

Pd nanoparticles with an average diameter of 2.2 nm were prepared by chemical reduction of $Pd(OAc)_2$, and the octadecanethiol molecules on the nanoparticle surface were exchanged with EDT-TTF(SCH_3)($SC_{10}H_{20}SH$) in solution. The molar proportion of TTF derivative in the organic layer can be varied from 0 to 75%. The magnetic susceptibility of the nanoparticles is expressed as the sum of the Curie term and the temperature-independent term. The Pauli paramagnetic susceptibility χ_0 of the Pd core after subtracting the core diamagnetism (Figure 5, a) is found to be only 12% of the Pauli susceptibility of bulk Pd (5.48×10^{-4} emu mol^{-1}). This result indicates that the quantum size and core-shell interface effects significantly modify the electronic structure of the Pd nanoparticle cores. Since the reduction of χ_0 due to the quantum size effect is expected to be similar for Pd and Pt nanoparticles of the same diameter, the major contribution in this larger reduction of Pauli paramagnetism in Pd nanoparticles comes from the interface effect. The bulk Pd metal has a sharp density-of-state peak around the Fermi level, which causes a large Pauli paramagnetic susceptibility.[12] The lowering of the Fermi level upon the core-to-shell charge transfer drastically reduces the density of states, which is reflected in the large reduction of the Pauli paramagnetic susceptibility.

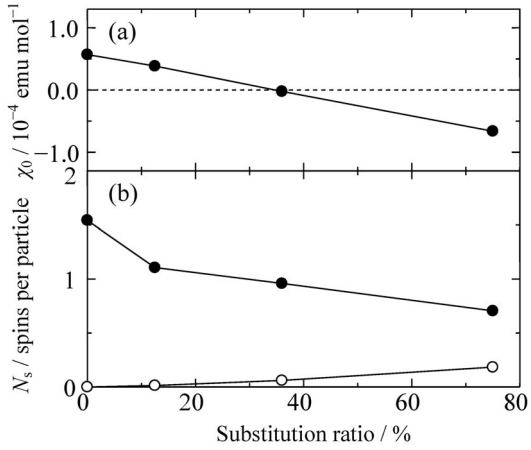

Figure 5. (a) The Pauli magnetic susceptibility χ_0 and (b) the spin concentration *Ns* as a function of the ratio of substitution by the TTF derivative molecule. The open circles denote the contribution of the TTF π-electrons.

As the surface octadecanethiol molecules are replaced with the TTF derivative molecules, the Pauli paramagnetic susceptibility χ_0 monotonically decreases and becomes negative when the substitution ratio exceeds 36% (Figure 5, a). XPS spectra show that the core Pd nanoparticles become more positive with the introduction of greater proportions of TTF. Before the exchange reaction with the TTF derivative, the spin concentration N_s per Pd nanoparticle is estimated to be 1.5, which is larger than that of Pt nanoparticles. The larger spin concentration is thought to be related to the strong paramagnetic features of Pd, which originate from the large density of states around the Fermi level. The substitution of octadecanethiol molecules with TTF derivative molecules reduces the localised spin concentration to 0.7 spins/particle at a TTF composition ratio of 75% (Figure 5, b). ESR spectra show that the spin concentration in the TTF derivative-substituted nanoparticle is actually a combination of contributions from the metal core and the TTF units, see open circles in Figure 5 (b). From the ESR signal intensity, the ratio of the TTF cation radical to the total number of TTF species is estimated to be on the order of 0.1%.

Single Particle Magnet Behaviour in Pd Nanoparticles Alloyed with a 3d-Transition Metal

As mentioned previously, palladium has been utilised as a useful material in magnetic functionalization due to its unique electronic properties. In the 1960s, Pd-based alloys such as Co-Pd,[13] Fe-Pd[27] and Ni-Pd[27] were intensively investigated in light of their giant magnetic moments. For example, the magnetic moments of Co atoms in Pd-based alloys are enhanced to ca. 10 times those of free Co atoms. Moriya explains this anomalous enhancement with an exchange enhancement theory.[14] In cases of normal metals where the electron correlation effect is negligible, the exchange interaction between the magnetic centres can be described with the Ruderman–Kittel–Kasuya–Yosida

(RKKY) mechanism[28] based on an uncorrelated free-electron model, in which the spin polarization of the conduction electron propagates from a magnetic centre with an oscillation (Figure 6). Moriya, however, takes the strong electron correlation of Pd into consideration and formulates the exchange interaction between Co localised electrons and Pd conduction electrons. In this theory, the spin polarization of the conduction electron decays monotonically as a function of the distance from the magnetic centre (Figure 6). This exchange enhancement theory is experimentally supported by a neutron scattering experiment in a Co-Pd alloy,[29] which clearly shows that the Pd atoms located within ca. 1 nm from the Co atom are ferromagnetically magnetised.

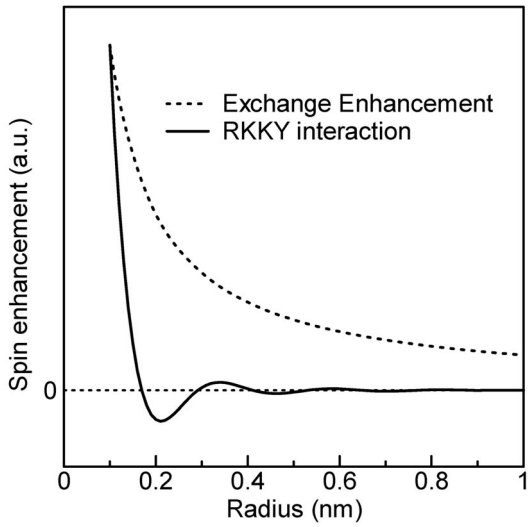

Figure 6. Spin polarization as a function of the distance from a magnetic centre according to the RKKY interaction and the exchange enhancement mechanism.

It is therefore of interest to see what would happen to the magnetic properties of these alloy systems by limiting the particle size to the same magnitude as that of the effective radius of the exchange enhancement mechanism. With this viewpoint as our impetus, we have investigated the magnetic properties of nanoparticles in a Co-Pd alloy system.[30]

Co-Pd nanoparticles were prepared by chemical reduction of $CoCl_2$ mixed with $Pd(OAc)_2$ using superhydride in the presence of octadecanethiol. The average diameter of the nanoparticles was controlled by carefully selecting the amount of octadecanethiol. TEM measurements revealed that all alloy nanoparticles took an fcc structure identical to that of bulk Pd regardless of their particle size. Co atoms are detected with a bulk elemental analysis (ICP-OES) but not with a surface-sensitive method (XPS), showing that Co atoms are located inside the Pd particles. Figure 7 shows the magnetic moment of alloy nanoparticles per Co atom as a function of Co concentration. The magnetic moment shows a sharp peak at 0.42 at-% Co atom. Interestingly, this concentration corresponds to that at which only a single Co atom is included in a Pd nanoparticle as the magnetic centre. Above 220 K, the magnetic moment of the nanoparticles is estimated be 9.4 μ_B. This value is nearly the same as that of bulk Co-Pd alloy (10 μ_B),[13] suggesting that a single Co atom can magnetise all Pd atoms inside a particle as a consequence of the exchange enhancement illustrated in Figure 8 (a).

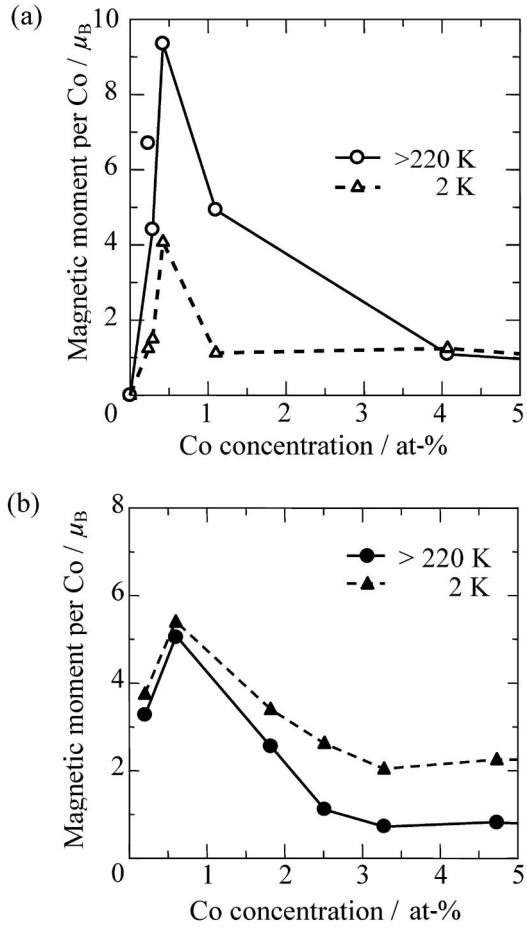

Figure 7. The Co concentration dependence of the magnetic moments of (a) 2-nm and (b) 3-nm Co-Pd alloy nanoparticles. The circles and triangles denote magnetic moments in the high- and low-temperature ranges, respectively.

The magnetic moment of the 2-nm alloy nanoparticle system at 2 K is smaller than the high-temperature magnetic moment above 220 K. This difference can be explained in terms of the quantum size effect. The energy discreteness $\delta \approx E_F/N$ of these particles is estimated to be ca. 20 meV from the Fermi energy of Pd and the particle size. Above the temperature $\delta/k_B \approx 200$ K, the conduction electrons of Pd are delocalised inside the nanoparticles, and the exchange enhancement mechanism works to elevate the magnetic moments of the Co magnetic centres. In the low-temperature region, the quantum size effect localises the conduction electrons of Pd. The exchange enhancement mechanism does not work effectively, resulting in the reduction of the magnetic moments.

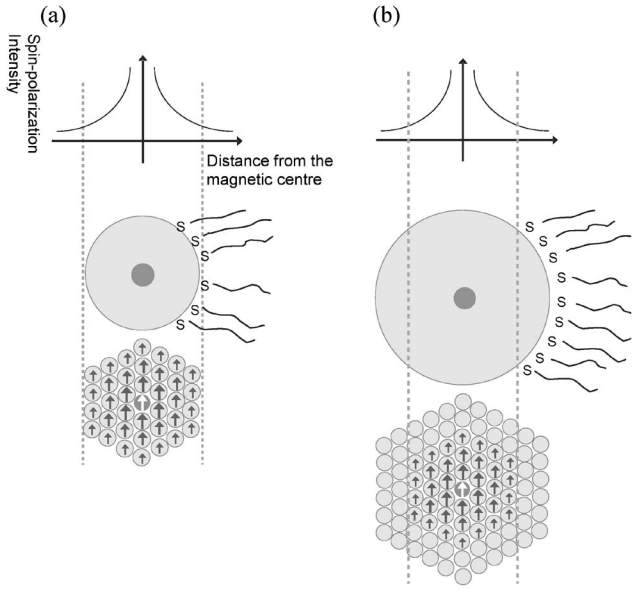

Figure 8. The exchange enhancement model for (a) 2-nm and (b) 3-nm Co-Pd alloy nanoparticles.

We next compared the magnetic properties of the two Co-Pd alloy nanoparticles with different particle diameters to elucidate the competition between the exchange enhancement mechanism and the quantum size effect. Compared to the quantum size effect for 2-nm alloy nanoparticles, that in a 3-nm alloy nanoparticle system turned out to be lower (Figure 7, b). Indeed, the magnetic moment of the 3-nm Co-Pd alloy nanoparticles at low temperatures (triangles) is close to that in the high-temperature range (circles), in contrast to the case of 2-nm alloy nanoparticles (Figure 7, a). It is therefore suggested that the quantum size effect, which reduces the exchange enhancement effect, is no longer effective in the larger 3-nm nanoparticle system, at least above 2 K.

The effect of the exchange enhancement can be compared between 2-nm and 3-nm Co-Pd alloy nanoparticles using magnetic moments in the high-temperature range. In the 2-nm system, the magnetic moment per Co atom attains a maximum value of 9.4 μ_B at 0.42 at-% of Co, a concentration where each nanoparticle contains one Co atom on average. In the 3-nm system, the maximum value occurs at 0.60 at-%, a concentration which corresponds to ca. 5 Co atoms per particle. At a lower concentration of 0.2 at-% (1–2 Co atoms per particle), the magnetic moment per Co atom is reduced to 3.3 μ_B. This trend is explained from the effective range of the exchange enhancement, which is estimated to be ca. 1 nm.[14,29] In the 2-nm alloy nanoparticle system, the effective range of the exchange enhancement fully covers a particle and every Pd atom inside the particle is magnetised by the Co atom (Figure 8, a). In the 3-nm alloy nanoparticles containing only one Co atom, the effective radius of the exchange enhancement is smaller than the particle radius. As a result, only a portion of the Pd atoms in the particle are magnetised by the Co atom (Figure 8, b).

We now discuss the magnetic properties of 2-nm Co-Pd alloy nanoparticles containing only one Co atom (0.42 at-%) in detail. The large magnetic moment indicates that the single Co atom ferromagnetically magnetises all Pd atoms in the particle. The magnetization of the 2-nm Co-Pd alloy nanoparticle system after field-cooling and after zero-field cooling below the blocking temperature of T_B = 3 K are clearly different (Figure 9). This is the typical blocking behaviour of superparamagnetic particles. From the blocking temperature and the particle volume, the effective uniaxial anisotropy (K_a) per unit volume of a single particle magnet is estimated to be 100 kJ m^{-3}. This value is comparable to the anisotropy of bulk Co (hcp: 450 kJ m^{-3}, fcc: 250 kJ m^{-3}),[31] and indicates a large magnetic anisotropy of the Co atom even in an extremely confined state.

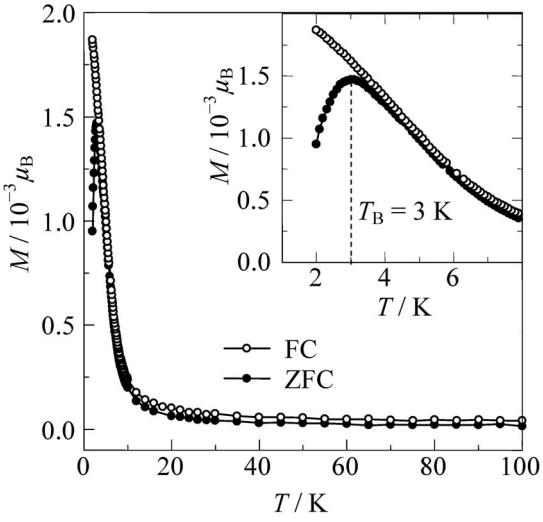

Figure 9. The temperature dependence of the magnetic moment in a single particle magnet of the 2-nm Co-Pd alloy nanoparticle (Co 0.42 at-%).

We can therefore refer to this Co-Pd alloy nanoparticle system as a "single particle magnet", which is defined similarly to single molecular magnets represented by Mn_{12} cluster systems.[32] All of the spins inside a particle or molecule are magnetically coupled together to form a single spin with a large spin multiplicity *S*. In the high-temperature range, this large spin rotates freely in the applied external magnetic field, similarly to conventional paramagnetic species. This spin reversal between preferred spin orientations is prohibited at low temperatures by an energy barrier produced by the axial magnetic anisotropy, resulting in blocking behaviour. One notable difference in the single particle magnet is the absence of quantum tunnelling between Zeeman sublevels, which is observed as stepwise magnetization curves in single-molecular magnets.[33] This indicates the semi-classical nature of a single particle magnet comprised of a Co-Pd alloy nanoparticle.

Conclusions

Metal nanoparticles coated with organic shells offer an intriguing architectural base with which a variety of magnetic functions can be created. With this idea in mind, we have developed novel magnetic systems based on alkanethiol-coated Pt and Pd nanoparticles using the quantum size, charge transfer and exchange enhancement effects as tools. The electron deficiency caused by the charge transfer from the metal core to the organic shell at the interface works to create localised magnetic moments. Substitution of simple alkanethiol molecules with TTF-substituted alkanethiol molecules having electron donating ability can modify the charge transfer at the interface, so that the electronic and magnetic features can be tuned in core/shell Pt/Pd nanoparticles.

When a 3d transition metal element such as Co is incorporated into Pd nanoparticles, their magnetic moment is significantly enhanced as a consequence of the exchange enhancement. As the particle size is comparable to the effective range of the exchange enhancement mechanism, a single Co atom can magnetise all of the Pd atoms in a 2-nm Co-Pd alloy nanoparticle. This results in single-particle magnetic behaviour involving superparamagnetic and blocking properties. A single particle magnet based on metal nanoparticles can potentially become a target of molecular magnetism and spintronics applications.[33] It is an intriguing building block in designing unconventional magnetic properties that cannot be obtained in either molecular or bulk systems.

Acknowledgments

We would like to thank Dr. Weixia Tu (Beijing University of Chemical Technology) who conducted the work on Pt and Pd nanoparticles, supported by the Japan Science Promotion Society (JSPS) Postdoctoral Fellowship for Foreign Researchers and the Natural Science Foundation of Young Teachers at the Beijing University of Chemical Technology (No. QN0401). A part of this work was supported by Grants-in-Aid for Scientific Research No. 12046231 and No. 15073211, the "Nanotechnology Support Project" of the Ministry of Education, Culture, Sports, Science and Technology (MEXT), Japan, Agency for Science, Technology and Research (ASTAR) Singapore, and a JSPS Fellowship.

[1] a) D. V. Talapin, J.-S. Lee, M. V. Kovalenko, E. V. Shevchenko, *Chem. Rev.* **2010**, *110*, 389–458; b) D. Tsoukalas, *Int. J. Nanotechnol.* **2009**, *6*, 35–45; c) D. Vanmaekelbergh, *Nat. Nanotechnol.* **2009**, *4*, 475–476.

[2] a) F. Wang, S.-S. Hu, *Microchimica Acta* **2009**, *165*, 1–22; b) H. Haick, *J. Phys. D* **2007**, *40*, 7173–7186.

[3] R. S. Ingram, M. J. Hostetler, R. W. Murray, T. G. Schaaff, J. T. Khoury, R. L. Whetten, T. P. Bigioni, D. K. Guthrie, P. N. First, *J. Am. Chem. Soc.* **1997**, *119*, 9279–9280.

[4] a) T. Sugawara, M. Minamoto, M. M. Matsushita, P. Nickels, S. Komiyama, *Phys. Rev. B* **2008**, *77*, 235316; b) S. Taniguchi, M. Minamoto, M. M. Matsushita, T. Sugawara, Y. Kawada, D. Bethell, *J. Mater. Chem.* **2006**, *16*, 3459–3465.

[5] a) R. Kubo, *J. Phys. Soc. Jpn.* **1962**, *17*, 975–986; b) R. Denton, B. Mühlschlegel, D. J. Scalapino, *Phys. Rev. B* **1973**, *7*, 3589–3607.

[6] a) N. A. Frey, S. Peng, K. Cheng, S.-H. Sun, *Chem. Soc. Rev.* **2009**, *38*, 2532–2542; b) A.-H. Lu, E. L. Salabas, F. Schüth, *Angew. Chem. Int. Ed.* **2007**, *46*, 1222–1244.

[7] M.-C. Daniel, D. Astruc, *Chem. Rev.* **2004**, *104*, 293–346.

[8] a) G. Schmid, R. Pfeil, R. Boese, F. Bandermann, S. Meyer, G. H. M. Calis, J. W. A. van der Velden, *Chem. Ber.* **1981**, *114*, 3634–3642; b) G. Schmid, M. Bäumle, M. Geerkens, I. Heim, C. Osemann, T. Sawitowski, *Chem. Soc. Rev.* **1999**, *28*, 179–185; c) G. Schmid, B. Corain, *Eur. J. Inorg. Chem.* **2003**, 3081–3098.

[9] a) M. Brust, M. Walker, D. Bethell, D. J. Schiffrin, R. J. Whyman, *J. Chem. Soc., Chem. Commun.* **1994**, 801–802; b) M. Brust, J. Fink, D. Bethell, D. J. Schiffrin, C. J. Kiely, *J. Chem. Soc., Chem. Commun.* **1995**, 1655–1656.

[10] J. M. Abad, S. F. L. Mertens, M. Pita, V. M. Fernández, D. J. Schiffrin, *J. Am. Chem. Soc.* **2005**, *127*, 5689–5694.

[11] H. Park, J. Yang, S. Seo, K. Kim, J. Suh, D. Kim, S. Haam, K.-H. Yoo, *Small* **2008**, *4*, 192–196.

[12] H. Chen, N. E. Nrener, J. Callaway, *Phys. Rev. B* **1989**, *40*, 1443–1449.

[13] R. M. Bozorth, P. A. Wolff, D. D. Davis, V. B. Compton, J. H. Wernick, *Phys. Rev.* **1961**, *122*, 1157–1160.

[14] T. Moriya, *Prog. Theor. Phys.* **1965**, *34*, 329–356.

[15] a) S. Gomez, K. Philippot, V. Collière, B. Chaudret, F. Senocq, P. Lecante, *Chem. Commun.* **2000**, 1945–1946; b) M. Green, P. A. O'Brien, *Chem. Commun.* **2000**, 183–184; c) J. Chen, L. Calvet, M. A. Reed, D. W. Carr, D. S. Grushiba, D. W. Bennett, *Chem. Phys. Lett.* **1999**, *313*, 741–748; d) H. S. Kim, S. J. Lee, N. H. Kim, J. K. Yoon, H.-K. Park, K. Kim, *Langmuir* **2003**, *19*, 6701–6710; e) W. Cheng, S. Dong, E. Wang, *Angew. Chem. Int. Ed.* **2003**, *42*, 449–452.

[16] a) A. Taleb, C. Petit, M. P. J. Pileni, *Phys. Chem. B* **1998**, *102*, 2214–2220; b) F. Chen, G.-Q. Xu, T. S. A. Hor, *Mater. Lett.* **2003**, *57*, 3282–3286; c) C.-L. Chiang, *J. Colloid Interf. Sci.* **2000**, *230*, 60–66; d) N. R. Jana, L. Gearheart, C. J. Murphy, *Adv. Mater.* **2001**, *13*, 1389–1393.

[17] a) S. T. Selvan, J. P. Spatz, H.-A. Klock, M. Möller, *Adv. Mater.* **1998**, *10*, 132–134; b) G. Carrot, J. C. Valmalette, C. J. G. Plummer, S. M. Scholz, J. Dutta, H. Hofmann, J. G. Hilborn, *Colloid Polym. Sci.* **1998**, *276*, 853–859.

[18] W. Tu, K. Takai, K. Fukui, A. Miyazaki, T. Enoki, *J. Phys. Chem. B* **2003**, *107*, 10134–10140.

[19] a) C. Yee, R. Jordan, A. Ulman, H. White, A. King, M. Rafailovich, J. Sokolov, *Langmuir* **1999**, *15*, 3486–3491; b) C. Yee, M. Scotti, A. Ulman, H. White, M. Rafailovich, J. Sokolov, *Langmuir* **1999**, *15*, 4314–4316.

[20] L. Pauling, *J. Am. Chem. Soc.* **1932**, *54*, 3570–3582.

[21] D. A. Gordon, R. F. Marzke, W. S. Glaunsinger, *J. Phys. Fr.* **1977**, *38*, C2–87–91.

[22] a) A. Kawabata, R. Kubo, *J. Phys. Soc. Jpn.* **1966**, *21*, 1765–1772; b) A. Kawabata, *J. Phys. Soc. Jpn.* **1970**, *29*, 902–911.

[23] a) R. J. Elliott, *Phys. Rev.* **1954**, *96*, 266–279; b) O. E. Andersson, B. L. V. Prasad, H. Sato, T. Enoki, Y. Hishiyama, Y. Kaburagi, M. Yoshikawa, S. Bandow, *Phys. Rev. B* **1998**, *58*, 16387–16395.

[24] W. Tu, K. Fukui, A. Miyazaki, T. Enoki, *J. Phys. Chem. B* **2006**, *110*, 20895–20900.

[25] a) S. Kagoshima, K. Kanoda, T. Mori (eds.), Organic Conductors, special topics section in *J. Phys. Soc. Jpn.* **2006**, *75*; b) P. Batail (Ed.), *Molecular Conductors*, special issue in: *Chem. Rev.* **2004**, *104*; c) T. Ishiguro, K. Yamaji, G. Saito, *Organic Superconductors*, Springer-Verlag, Heidelberg, Germany, **1998**.

[26] a) M. R. Bryce, *Chem. Soc. Rev.* **1991**, *20*, 335–390; b) J. Roncali, *J. Mater. Chem.* **1997**, *7*, 2307–2321.

[27] J. Crangle, W. R. Scott, *J. Appl. Phys.* **1965**, *36*, 921–928.

[28] a) M. A. Ruderman, C. Kittel, *Phys. Rev.* **1954**, *96*, 99–102; b) T. Kasuya, *Prog. Theor. Phys.* **1956**, *16*, 45–57; c) K. Yosida, *Phys. Rev.* **1957**, *106*, 893–898.

[29] G. G. Low, T. M. Holden, *Proc. Phys. Soc.* **1966**, *89*, 119–127.

[30] Y. Ito, A. Miyazaki, K. Fukui, S. Valiyaveettil, T. Yokoyama, T. Enoki, *J. Phys. Soc. Jpn.* **2008**, *77*, 103701.
[31] R. E. Newnham, *Properties of Materials: Anisotropy, Symmetry, Structure*, Oxford University Press, Oxford, **2005**.
[32] a) D. Gatteschi, R. Sessoli, *Angew. Chem. Int. Ed.* **2003**, *42*, 268–297; b) M. R. Pederson, S. N. Khanna, *Phys. Rev. B* **1999**, *60*, 9566–9572; c) A. M. Gomes, M. A. Novak, R. Sessoli, A. Caneschi, D. Gatteschi, *Phys. Rev. B* **1998**, *57*, 5021–5024.
[33] a) A. Lu, E. L. Salabas, F. Schüth, *Angew. Chem. Int. Ed.* **2007**, *46*, 1222–1244; b) O. Waldmann, *Coord. Chem. Rev.* **2005**, *249*, 2550–2566; c) X. Batlle, A. Labarta, *J. Phys. D: Appl. Phys.* **2002**, *35*, R15–R42.

Received: April 30, 2010
Published Online: August 16, 2010

